9858–9872 *Nucleic Acids Research, 2022, Vol. 50, No. 17* *Published online 12 September 2022*
https://doi.org/10.1093/nar/gkac770

Formation and removal of 1,N^6-dimethyladenosine in mammalian transfer RNA

Xue-Jiao You[1,2,3,†], Shan Zhang[1,2,†], Juan-Juan Chen[2], Feng Tang[2], Jingang He[4,5], Jie Wang[4,5], Chu-Bo Qi[6], Yu-Qi Feng[1,2] and Bi-Feng Yuan[1,2,3,*]

[1]Department of Radiation and Medical Oncology, Cancer Precision Diagnosis and Treatment and Translational Medicine Hubei Engineering Research Center, Zhongnan Hospital of Wuhan University, School of Public Health, Wuhan University, Wuhan 430071, China, [2]Sauvage Center for Molecular Sciences, Department of Chemistry, Wuhan University, Wuhan 430072, China, [3]Wuhan Research Center for Infectious Diseases and Cancer, Chinese Academy of Medical Sciences, Wuhan 430071, China, [4]State Key Laboratory of Magnetic Resonance and Atomic and Molecular Physics, National Center for Magnetic Resonance in Wuhan, Wuhan Institute of Physics and Mathematics, Innovation Academy for Precision Measurement Science and Technology, Chinese Academy of Sciences-Wuhan National Laboratory for Optoelectronics, Wuhan 430071, China, [5]University of Chinese Academy of Sciences, Beijing, China and [6]Department of Pathology, Jiangxi Provincial People's Hospital, The First Affiliated Hospital of Nanchang Medical College, Nanchang 330006, China

Received April 09, 2022; Revised August 17, 2022; Editorial Decision August 18, 2022; Accepted August 27, 2022

ABSTRACT

RNA molecules harbor diverse modifications that play important regulatory roles in a variety of biological processes. Over 150 modifications have been identified in RNA molecules. N^6-methyladenosine (m^6A) and 1-methyladenosine (m^1A) are prevalent modifications occurring in various RNA species of mammals. Apart from the single methylation of adenosine (m^6A and m^1A), dual methylation modification occurring in the nucleobase of adenosine, such as N^6,N^6-dimethyladenosine ($m^{6,6}A$), also has been reported to be present in RNA of mammals. Whether there are other forms of dual methylation modification occurring in the nucleobase of adenosine other than $m^{6,6}A$ remains elusive. Here, we reported the existence of a novel adenosine dual methylation modification, i.e. 1,N^6-dimethyladenosine ($m^{1,6}A$), in tRNAs of living organisms. We confirmed that $m^{1,6}A$ is located at position 58 of tRNAs and is prevalent in mammalian cells and tissues. The measured level of $m^{1,6}A$ ranged from 0.0049% to 0.047% in tRNAs. Furthermore, we demonstrated that TRMT6/61A could catalyze the formation of $m^{1,6}A$ in tRNAs and $m^{1,6}A$ could be demethylated by ALKBH3. Collectively, the discovery of $m^{1,6}A$ expands the diversity of RNA modifications and may elicit a new tRNA modification-mediated gene regulation pathway.

GRAPHICAL ABSTRACT

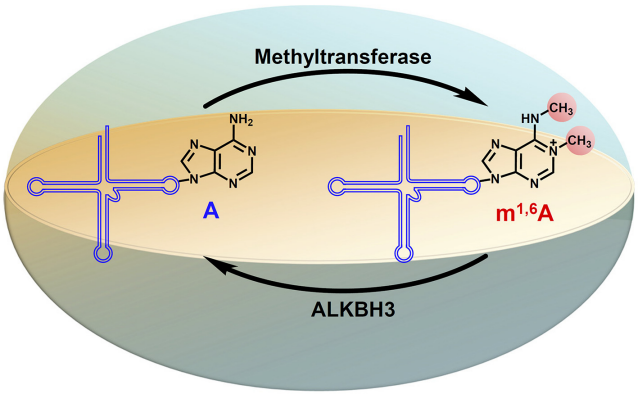

INTRODUCTION

Beyond the four canonical nucleobases, RNA molecules also carry a diverse array of modifications (1). In recent years, there have been substantial efforts to uncover and characterize the modifications present on RNA, motivated by the potential of such modifications to regulate RNA metabolism (2). Over 150 different types of modifications have been reported to be present in various RNA species across all domains of living organisms (3). These naturally occurring modifications in RNA molecules serve critical roles in impacting RNA structure and also broaden our understanding toward the functions of RNA molecules (4–6). In a manner analogous to DNA, increasing evidence

*To whom correspondence should be addressed. Tel: +86 27 68788762; Fax: +86 27 68788762; Email: bfyuan@whu.edu.cn
†The authors wish it to be known that, in their opinion, the first two authors should be regarded as Joint First Authors.

proposes that these modifications in RNA molecules participate in regulating RNA processes (7).

Methylation is the most prevalent modification occurring in RNA molecules of mammals (3). Two isomeric adenosine methylation modifications of N^6-methyladenosine (m^6A) and 1-methyladenosine (m^1A) have been reported to be widely present in different RNA species of mammals (8). m^6A is found in eukaryotic messenger RNA (mRNA), transfer RNA (tRNA), ribosomal RNA (rRNA) and non-coding RNA (ncRNA) (9). Intensive studies of m^6A in recent years have implicated m^6A in a broad range of critical functions, ranging from cell development and differentiation (10), stress responses (11,12), to development of cancers (13). At the molecular level, m^6A is involved in RNA stability (14), regulation of translation (15), and microRNA biogenesis (16). m^1A is a modification primarily observed in the conserved sites in rRNA and tRNA (17–19). m^1A is also found in mammalian mRNA, with enrichment in the 5′ untranslated region (5′ UTR) (20–22). m^1A in RNA can affect ribosome biogenesis, respond to environmental stress, and mediate antibiotic resistance in bacteria (23).

Apart from the single methylation on the nucleobase of adenosine (m^6A and m^1A), dual methylation modification occurring in the nucleobase of adenosine, such as N^6,N^6-dimethyladenosine ($m^{6,6}A$), also has been reported to be present in RNA. $m^{6,6}A$ is a conserved modification found in human 18S rRNA and plays a critical role in ribosome biogenesis (24,25). Since both m^1A and m^6A are ubiquitous modifications in RNA of mammals, we speculate that the dimethylated adenosine other than $m^{6,6}A$, such as 1,N^6-dimethyladenosine ($m^{1,6}A$), may be present in RNA. However, unlike $m^{6,6}A$, $m^{1,6}A$ has never been discovered in living organisms across the three-domain system, including archaea, bacteria, and eukaryotes. The presence of $m^{1,6}A$ in RNA remains an open question.

In this study, we reported the existence of a novel adenosine dual methylation modification, i.e. $m^{1,6}A$, in tRNAs of mammalian cells and tissues. Notably, we demonstrated that $m^{1,6}A$ was located at position 58 of tRNAs. Furthermore, we demonstrated that TRMT6/61A was responsible for the formation of $m^{1,6}A$ in tRNAs and ALKBH3 was capable of demethylating $m^{1,6}A$ in tRNAs.

MATERIALS AND METHODS

Chemicals and reagents

The nucleosides and modified nucleosides, including adenosine (A), guanosine (G), cytidine (C), uridine (U), *N*3-methylcytidine (m^3C), 5-methylcytidine (m^5C), *N*7-methylguanosine (m^7G), N^6-methyladenosine (m^6A), N^6,N^6-dimethyladenosine ($m^{6,6}A$), 1-methyladenosine (m^1A), 1,2′-*O*-dimethyladenosine (m^1Am), and N^6,2′-*O*-dimethyladenosine (m^6Am) were purchased from various commercial sources and the detailed information of these nucleosides can be found in Supplementary Table S1 in Supporting Information. 1,N^6-dimethyladenosine ($m^{1,6}A$) was synthesized in the current study. Venom phosphodiesterase I and TRIzol reagent were purchased from Sigma-Aldrich (Beijing, China). Calf intestinal alkaline phosphatase (CIAP) and S1 nuclease were obtained from Takara Biotechnology (Dalian, China). Proteinase K was obtained from Sangon Biotechnology (Shanghai, China). Dimethyl sulfate (DMS) was purchased from Macklin Biochemical Technology Co., Ltd (Shanghai, China). Trimethylsulfoniumiodide (Me_3SI) was purchased from Bide Pharmatech Ltd. (Shanghai, China). L-Methionine-(methyl-D_3) (D_3-Met) was purchased from Aladdin Industrial Inc. (Shanghai, China). Dulbecco's modified Eagle's medium (DMEM), RPMI-1640 medium and fetal bovine serum were purchased from Thermo-Fisher Scientific (Beijing, China). Chromatographic grade methanol was purchased from Merck (Darmstadt, Germany).

Synthesis and characterization of $m^{1,6}A$

$m^{1,6}A$ was synthesized by two different strategies. Briefly, 20 μM of m^1A or m^6A was used as the substrate to react with 100 mM of DMS under different pH at 37°C for 1 h. Alternatively, m^6A (6 mg) in DMF was used as the substrate to react with Me_3SI (30 mg) at 85°C for 3.5 h. The obtained $m^{1,6}A$ was separated and purified by high performance liquid chromatography (HPLC). The HPLC separation was performed on Shimadzu LC-20AT HPLC system. A homemade C18-T column (10.0 × 250 mm) was employed for the separation. An isocratic separation was performed at a flow rate of 2.0 ml/min with 10% methanol (v/v) as the mobile phase. The synthesized $m^{1,6}A$ was characterized by high-resolution mass spectrometry and nuclear magnetic resonance (NMR) analysis.

Biological and clinical samples

Human embryonic kidney 293T cell line (HEK293T), human cervical carcinoma cell line (HeLa), human hepatic cell line (HL-7702), human breast cancer cell line (MCF-7), human liver carcinoma cell line (HepG2), human malignant myeloid cell line (K562), human leukemic cell line (Jurkat-T), and mouse neuroblastoma N2a cell line (Neuro-2a) were obtained from the China Center for Type Culture Collection. HEK293T, HeLa, MCF-7, HepG2 and Neuro-2a cells were grown in DMEM medium. HL-7702, Jurkat-T and K562 cells were grown in RPMI-1640 medium. The medium was supplemented with 10% fetal bovine serum, 100 U/mL penicillin, and 100 μg/mL streptomycin. Cells were maintained in a humidified atmosphere with 5% CO_2 at 37°C. As for stable isotope tracing experiments, human HEK293T and HeLa cells were cultured in DMEM medium supplemented with 0.3 mM of D_3-Met. HEK293T and HeLa cells were harvested after culturing for 72 h in DMEM medium supplied with D_3-Met.

The animal experiment was treated in accordance with the protocols and approved by the Animal Ethics Committee at the Innovation Academy for Precision Measurement Science and Technology, Chinese Academy of Sciences. The rat and mouse were anesthetized and euthanized, and the rat brain tissues were quickly removed and manually divided into nine regions, including olfactory bulb (OB), cerebellum (CE), medulla (MED), midbrain (MID), thalamus (THA), hypothalamus (HYP), hippocampus (HP), striatum (ST) and cerebral cortex (CC). A total of 10 breast cancer tissues and matched tumor-adjacent normal tissues from five breast cancer patients were collected from Hubei

Cancer Hospital. The human related study was granted and approved by the Hubei Cancer Hospital Ethics Committee and met the declaration of Helsinki. All the experiments were performed in accordance with Hubei Cancer Hospital Ethics Committee's guidelines and regulations.

Purification of different RNA species

Cellular total RNA was extracted using TRIzol reagent (Sigma-Aldrich, Beijing, China) according to the manufacturer's recommended procedure. Large RNA (>200 nt) and small RNA (<200 nt) were purified using an E.Z.N.A. miRNA kit (Omega Bio-Tek Inc., Norcross, GA, USA). The small RNA (<200 nt) was further separated by 10% urea–PAGE and gel-purified to obtain tRNAs, 5S rRNA and 5.8S rRNA. For the isolation of 18S rRNA and 28S rRNA, the total RNA was further separated by means of size exclusion chromatography (SEC) using a Bio SEC-5 column (5 mm, 1000 Å, 4.6 × 150 mm; Agilent Technologies, Foster City, CA, USA) according to a previous study (26). Isocratic separation was performed at a flow rate of 0.35 ml/min at 35°C with 100 mM CH_3COONH_4 (pH 7.0) as the mobile phase. The fraction was collected and processed with the E.Z.N.A. miRNA kit to remove salt. For mRNA isolation, the obtained large RNA (>200 nt) was extracted twice using PolyATtract® mRNA isolation system (Promega, Madison, WI, USA). The isolated RNA was quantified by UV spectrophotometer B-500 (Metash, Shanghai, China).

Isolation of individual tRNA

Typically, 20 μl of PuriMag G-Streptavidin magnetic beads (PuriMag Biotech, Xiamen, China) were washed three times with 1× binding buffer (20 mM Tris–HCl, pH 8.0, 0.5 M NaCl), and then resuspended in 100 μl of 1 × binding buffer. Subsequently, 40 μM of biotin-labeled DNA probe (Supplementary Table S2 in Supporting Information) that is complementary to individual tRNA in 100 μl of 1× binding buffer was added to beads and incubated at 25°C for 30 min with gentle mixing. The DNA probe-coated beads were then washed four times using 200 μl of 1× binding buffer and resuspended in 100 μl of 1× binding buffer. Then 30 μg of purified tRNAs dissolved in 100 μl of 1× binding buffer was mixed with the DNA probe-coated beads and incubated at 75°C for 10 min followed by incubation at 25°C for 3 h to allow the hybridization of the individual tRNA to DNA probe. The DNA probe-coated beads were washed five times with 200 μl of washing buffer (7 mM Tris–HCl, pH 8.0, 0.17 M NaCl). The individual tRNA was recovered by degradation of streptavidin with 27 μM of proteinase K digestion at 55°C for 40 min in 50 μl of RNase-free H_2O or through incubation in 20 μl buffer (95% formamide, 10 mM EDTA, pH 8.2) at 65°C for 5 min. The resulting tRNA was further purified using RNA Clean & Concentrator kit (Zymo Research).

Isolation of specific fragment of tRNA

To obtain a specific fragment of tRNA, we proposed a strategy of DNA hybridization protection combined with S1 nuclease digestion. Specifically, 600 ng of purified $tRNA^{Gly(GCC)}$ and 5 μM of 22-mer biotin-labeled DNA probe (or 20-mer or 18-mer biotin-labeled DNA probe, Supplementary Table S2 in Supporting Information) were mixed in a 20-μl of hybridization buffer (50 mM Tris–HCl, pH 7.0, 5 mM $MgCl_2$). The mixture was heated at 70°C for 10 min followed by gradual cooling down to 25°C to allow the hybridization of the 22-mer biotin-labeled DNA probe (or 20-mer or 18-mer biotin-labeled DNA probe) with $tRNA^{Gly(GCC)}$. Subsequently, S1 nuclease (180 units/μl in stock solution) was added to the mixture (final concentration of 0.3 units/μl) to digest the single-stranded region of $tRNA^{Gly(GCC)}$ as well as the excess biotin-labeled DNA probe at 23°C for 15 min. Finally, the PuriMag G-Streptavidin magnetic beads were applied for isolation of the 22-bp RNA/DNA hybrid (or 20-bp or 18-bp RNA/DNA hybrid) according to the aforementioned procedure.

LC–ESI-MS/MS analysis

RNA was enzymatically digested under neutral conditions according to our previously described method (27). LC–ESI-MS/MS analysis of the digested nucleosides was performed on a Shimadzu 8045 mass spectrometer (Kyoto, Japan) equipped with an electrospray ionization (ESI) source (Turbo Ionspray) and a Shimadzu LC-30AD UPLC system (Tokyo, Japan). A Shimadzu Shim-pack GIST C18 column (100 mm × 2.1 mm i.d., 2.0 μm) was employed for the separation at 40°C. The mobile phases consist of 0.05% formic acid/H_2O (solvent A) and methanol (solvent B) with a flow rate of 0.2 ml/min. A 20-min gradient (0−2 min of 5% B, 2−10 min of 5 to 80% B, 10−12 min of 80% B, 12−13 min of 80 to 5% B and 13–20 min of 5% B) was employed for the separation. The nucleosides were detected by multiple reaction monitoring (MRM) under positive-ion mode. The optimal MRM mass spectrometric parameters are listed in Supplementary Table S3 in Supporting Information.

High-resolution mass spectrometry analysis

The synthesized $m^{1,6}A$ was characterized using a high-resolution LTQ-Orbitrap Elite mass spectrometer (Thermo Fisher Scientific, Waltham, MA, USA), which was equipped with an ESI source and a Dionex Ultimate 3000 UPLC system (Thermo Fisher Scientific, Waltham, MA, USA). The LC separation conditions were the same as that on Shimadzu 8045 mass spectrometer system. The MS analysis was performed in positive-ion mode with full scan detection (m/z 100–350) at a resolution of 60 000. The molecular mass (m/z 296.1) of the $m^{1,6}A$ was listed as the precursor ions for MS/MS analysis. The high-resolution MS/MS analysis was performed under positive-ion mode at the resolution of 60000 using collision induced dissociation (CID) activation mode with a collision energy of 20 eV. In addition, the product ion (m/z 164.1) of the $m^{1,6}A$ was listed as the precursor ions for MS^3 analysis. The high resolution MS^3 analysis was performed under positive-ion mode at the resolution of 60 000 using CID activation mode with a collision energy of 35 eV. The source and ion transfer parameters applied were as follows: capillary

temperature, 350°C; heater temperature, 300°C; auxiliary gas flow, 15 arbitrary units; sheath gas flow, 35 arbitrary units; capillary voltage, 35 V; spray voltage, 3.5 kV; the S-lens RF level, 60%. Data analysis was performed using Xcalibur v3.0.63 (Thermo Fisher Scientific, Waltham, MA, USA).

Expression and purification of recombinant proteins

The human *ALKBH3* (*hALKBH3*), human *ALKBH1* (*hALKBH1*), human *TRMT6* (*hTRMT6*), human *TRMT61A* (*hTRMT61A*) and mouse *Alkbh3* (*mAlkbh3*) genes were synthesized by TsingKe Biological Technology (Beijing, China). The synthesized *hALKBH3*, *hALKBH1*, *hTRMT6* and *mAlkbh3* genes were separately cloned into pGEX-4T1 plasmid that contains the glutathione S-transferase (GST) tag. The *hTRMT61A* gene was inserted into pET28(a) plasmid. The human *METTL16* gene was constructed from the MTase domain (1–310 amino acids, referred to as *hMTD16*) and inserted into pET28(a) plasmid. These protein-expressing constructs were examined and confirmed by sequencing and transformed into BL21 (DE3) strain, grown in LB medium at 37°C until the OD600 reached 0.8−1.2. As for the expression of the hTRMT6/61A protein complex, the protein-expressing constructs for TRMT6 and TRMT61A were simultaneously transformed into BL21 (DE3) strain. The induced protein expression was carried out at 16°C for 20 h with the addition of 0.5 mM IPTG (isopropyl-β-D-thiogalactopyranoside).

For the purification of hALKBH1, hALKBH3 and mALKBH3 proteins, *E. coli* cells were collected in PBS buffer (136 mM NaCl, 2.6 mM KCl, 8 mM Na_2HPO_4, 2 mM KH_2PO_4, 2 mM DTT) supplemented with protease inhibitors (0.2 mM). After ultrasonication, the supernatant was applied to purify recombinant proteins using GST affinity beads. After washing with PBS buffer, Cryonase™ Cold-Active nuclease (Takara Biotechnology, Dalian, China) was added to degrade the residual nucleic acid at 4°C for 1 h. The recombinant proteins were eluted with 20 mM reduced glutathione in 100 mM Tris–HCl (pH 8.0). For the purification of hMTD16, *E. coli* cells were collected in the lysis buffer (20 mM Tris–HCl 8.0, 150 mM NaCl), and the recombinant protein was purified using Ni-NTA and then eluted with 250 mM imidazole in the elution buffer (20 mM Tris–HCl, pH 8.0, 150 mM NaCl). For the purification of hTRMT6/61A protein complex, we used GST affinity beads to pulldown the complex followed by elution with 20 mM reduced glutathione in 100 mM Tris–HCl (pH 8.0). All the purified proteins were analyzed by SDS-PAGE and stored at –80°C.

In vitro methylation and demethylation assay

The *in vitro* methylation and demethylation assays were conducted according to previous studies with slight modifications (28,29). For the methylation assay of hMTD16, the reaction mixture (20 μl) contained 50 mM Tris–HCl (pH 8.0), 200 mM NaCl, 2 mM $MgCl_2$, 1 mM DTT, 0.2 units/μl (final concentration) of RNase inhibitor, 1 mM SAM (*S*-adenosyl-L-methionine), 20 μM hMTD16, and 5 pmol hairpin RNA (Supplementary Table S2 in Supporting Information) or 100 ng of purified tRNAs. The reaction was carried out at 37°C for 3 h. For the methylation assay of hTRMT6/61A, the mixture (20 μl) included 50 mM Tris–HCl (pH 8.0), 50 mM NH_4Cl, 10 mM $MgCl_2$, 1 mM DTT, 0.2 units/μl (final concentration) of RNase inhibitor, 60 μM SAM, 5 μM hTRMT6/61A, and 200 ng of tRNAs. The reaction was performed at 30°C for different times. For the demethylation assay, the reaction solution (20 μl) contained 10 μM recombinant hALKBH1, hALKBH3 or mALKBH3 protein, 600 ng of purified tRNAs, 100 mM KCl, 2 mM $MgCl_2$, 0.2 units/μl (final concentration) of RNase inhibitor, 2 mM L-ascorbic acid, 1 mM α-ketoglutarate, 150 μM $(NH_4)_2Fe(SO_4)_2{\cdot}6H_2O$, and 50 mM Tris–HCl (pH 7.0). The reaction was carried out at 37°C for 3 h. All the reactions were quenched by heating at 95°C for 5 min.

Overexpression and siRNA knockdown

The plasmid pEGFP N1-hALKBH1, pCMV Sport6-hALKBH3, and pCMV Sport6-mALKBH3 were obtained from Sangon Biotechnology (Shanghai, China) and confirmed by sequencing. Human HEK293T cells were transfected with these plasmids or control plasmids using Lipofectamine 3000 (Invitrogen, USA) according to the manufacturer's instruction. Knockdown of *hALKBH1* or *hALKBH3* was performed using siRNA (TsingKe Biological Technology, Beijing, China) targeting human *ALKBH1* or *ALKBH3* mRNA. The non-targeting siRNA was used as a negative control. The sequences of *hALKBH1*, *hALKBH3* siRNA and control siRNA are listed in Supplementary Table S2 in Supporting Information. Human HEK293T cells were transfected with *hALKBH1* siRNA, *hALKBH3* siRNA, or control siRNA using Lipofectamine 2000 (Invitrogen, USA) according to the manufacturer's instruction. The culture medium was changed at 8 h after transfection and cells were harvested at 48 h after transfection.

Quantitative real-time PCR analysis

The isolated total RNA (1 μg) was used to generate cDNA using Hifair®**III** 1st Strand cDNA Synthesis SuperMix for qPCR (gDNA digester plus) (Yeasen Biotechnology, Shanghai, China). The Hieff® qPCR SYBR Green Master mix (No Rox) (Yeasen Biotechnology, Shanghai, China) was used for PCR reaction according to the manufacturer's instructions. Quantitative real-time PCR (qPCR) was performed using a CFX96 Real-Time PCR Detection system (Bio-Rad Laboratories). The levels of gene expression were normalized to glyceraldehyde 6-phosphate dehydrogenase gene (*GAPDH*). The sequences of PCR primers are listed in Supplementary Table S2 in Supporting Information.

Western blotting

HEK293T cells were lysed using RIPA lysis buffer (Beyotime Biotechnology, Shanghai, China). Then proteins were analyzed by SDS-PAGE and transferred to a PVDF

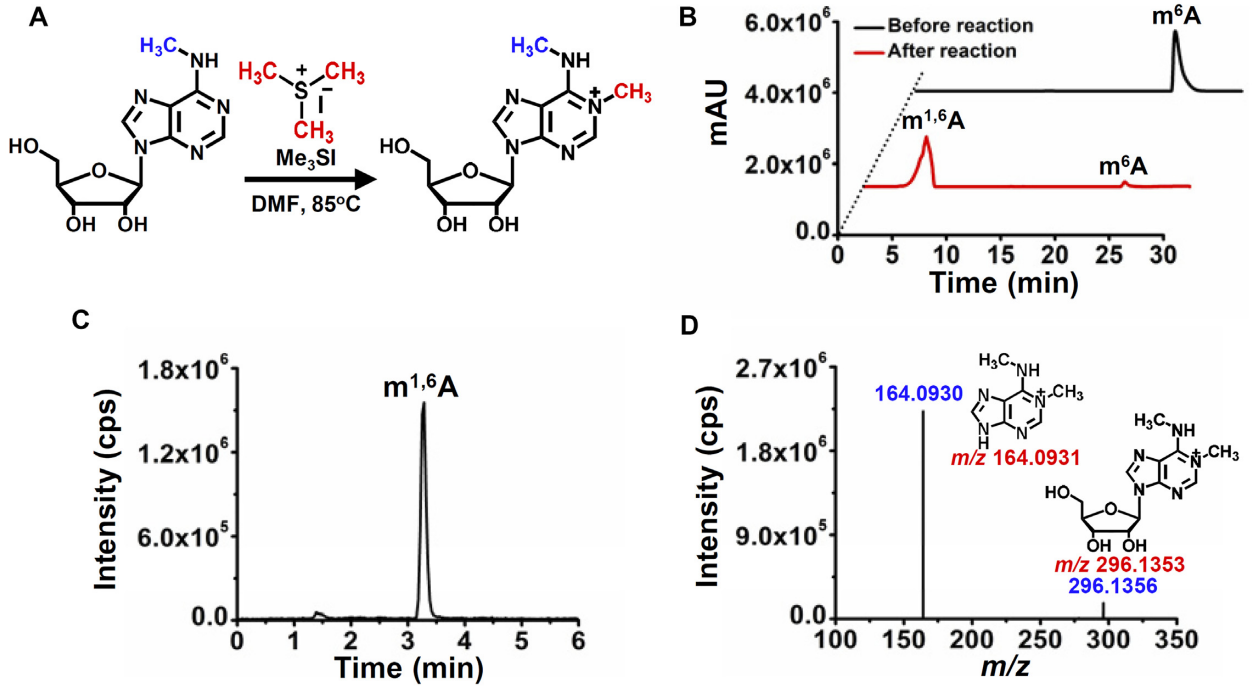

Figure 1. Synthesis and characterization of $m^{1,6}A$ by high-resolution mass spectrometry. (**A**) The chemical reaction for the synthesis of $m^{1,6}A$. (**B**) Chromatogram for separation and purification of $m^{1,6}A$. (**C**) The extracted-ion chromatogram of the synthesized $m^{1,6}A$. (**D**) MS/MS spectra of the synthesized $m^{1,6}A$ by high-resolution mass spectrometry analysis. Shown in red are theoretical m/z; shown in blue are measured m/z.

membrane (Millipore). Membranes were blocked with 5% milk proteins in TBST buffer (50 mM Tris–HCl pH 7.6, 150 mM NaCl and 0.1% Tween-20), and probed with primary antibody for 2 h. Then the membranes were washed three times with TBST buffer (5 min each) and probed with HRP-conjugated secondary antibody for 1 h. After washing three times, signal was detected using ECL western blot kit (ComWin Biotech Co., Ltd., Beijing, China) and imaged on a Tanon-4600SF chemiluminescent detector (Tanon, Shanghai, China). Antibodies that specifically recognized ALKBH1 (Abcam, ab12889, Cambridge, MA), ALKBH3 (Abcam, ab93174, Cambridge, MA) and GAPDH (Cell Signaling Technology, Danvers, MA) were used at 1:2000, 1:2000 and 1:3000 dilutions, respectively. HRP-conjugated secondary goat anti-rabbit antibody (Abcam, ab6721, Cambridge, MA) was used at a 1:10 000 dilution.

RESULTS AND DISCUSSION

Characterization of the synthesized $m^{1,6}A$

m^1A and m^6A are two prevalent modifications in RNA of mammals. In addition to the single methylation of adenine, dual methylation of adenine, such as $m^{6,6}A$, has also been identified to be present in RNA of mammals. However, the dual methylation of adenine, i.e. $m^{1,6}A$, has not been reported before. In this study, we aimed to investigate whether $m^{1,6}A$ is present in RNA of mammals.

We first synthesized the $m^{1,6}A$ standard, which is essential for the unambiguous determination of its potential presence in RNA of mammals. It has been reported that DMS can methylate the N1 or N6 position of adenosine under different pH conditions (30). Thus, we initially used m^1A and m^6A as the substrates to react with DMS to synthesize $m^{1,6}A$ (Supplementary Figures S1 and S2 in Supporting Information). The results showed that the potential $m^{1,6}A$ could be obtained; however, the yield was low. We therefore carried out the reaction under different pH to test whether pH plays critical role on the reaction efficiency for the synthesis of $m^{1,6}A$. However, the yield of $m^{1,6}A$ was still low and many by-products were also produced under different reaction conditions (Supplementary Figures S1 and S2 in Supporting Information). It can be seen that the reaction is not suitable for the synthesis of $m^{1,6}A$ standard. In this respect, we turned to use Me_3SI as the reagent to react with m^6A (Figure 1A). The HPLC analysis showed that, in addition to the substrate of m^6A (24.0 min), a new peak occurred at 5.0 min after the reaction (Figure 1B). The yield for $m^{1,6}A$ is estimated to be ~90%. The high-resolution MS analysis showed that the precursor ion (m/z 296.1356) and fragment ions (m/z 164.0930) of the synthesized product were identical to the theoretical m/z of $m^{1,6}A$ (m/z 296.1353 and 164.0931, Figure 1C and D), indicating that the compound should be the desired $m^{1,6}A$. The chromatographic retention time of this synthesized compound (3.2 min) in LC–ESI-MS/MS analysis is different from that of $m^{6,6}A$ standard (7.8 min) (Supplementary Figure S3 in Supporting Information), excluding the possibility of the synthesized compound being $m^{6,6}A$. In addition, NMR analysis further confirmed the synthesized compound was $m^{1,6}A$ (Supplementary Figures S4–S6 in Supporting Information). Collectively, these results demonstrated that $m^{1,6}A$ was successfully synthesized with high yield by using Me_3SI as the reagent.

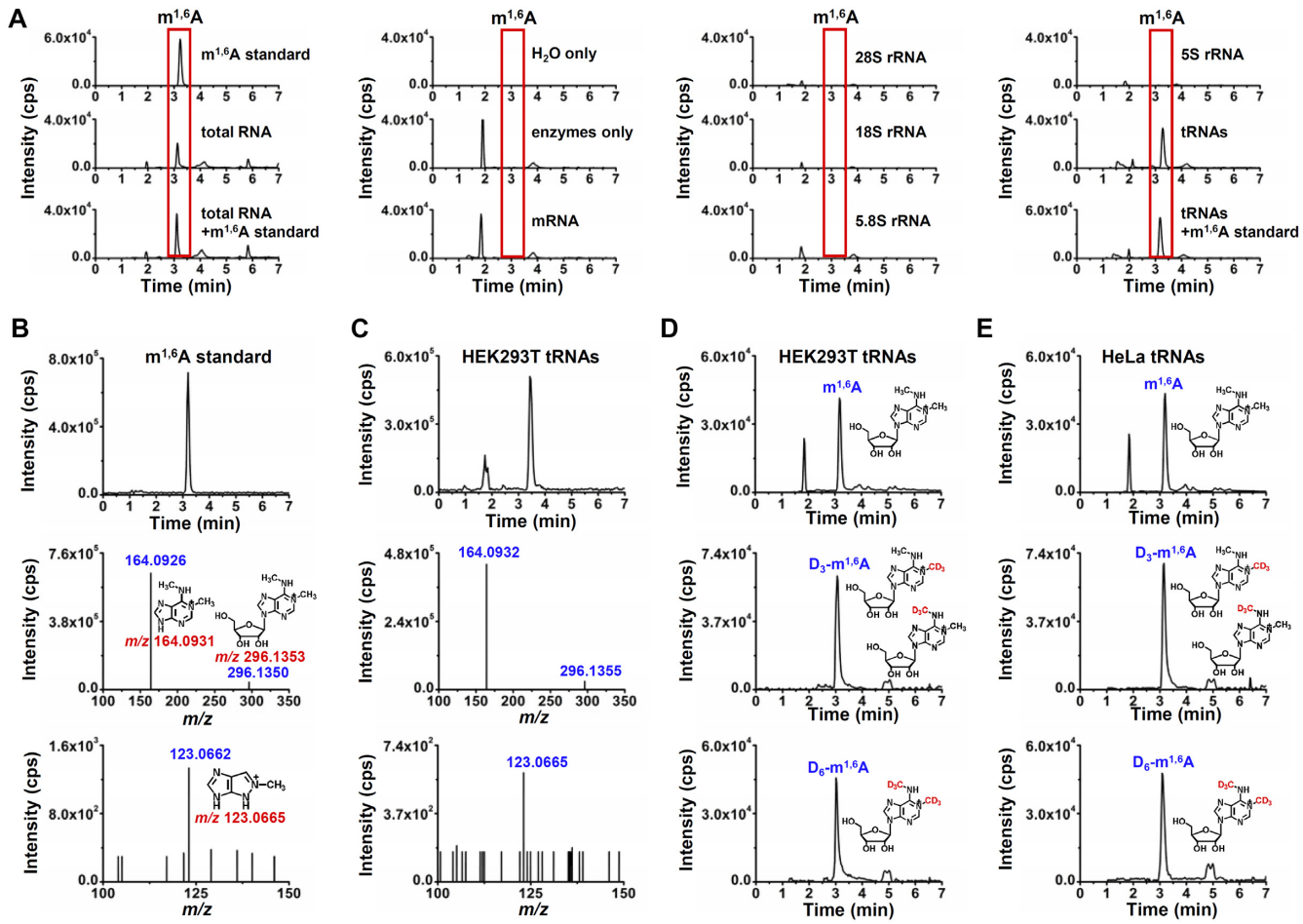

Figure 2. Determination of $m^{1,6}A$ in mammalian tRNAs. (**A**) The extracted-ion chromatograms of $m^{1,6}A$ from different samples by LC-ESI-MS/MS analysis. The synthesized $m^{1,6}A$ standard was added into the enzymatically digested total RNA or tRNAs of HEK293T cells to confirm the existence of $m^{1,6}A$. (**B**, **C**) Confirmation of the detected $m^{1,6}A$ from tRNAs of HEK293T cells by high-resolution mass spectrometry analysis. The extracted-ion chromatograms (upper panel), MS/MS spectra (middle panel), and MS^3 spectra (bottom panel) of the synthesized $m^{1,6}A$ standard and detected $m^{1,6}A$ from tRNAs of HEK293T cells. (**D**, **E**) Identification of $m^{1,6}A$ in tRNAs of HEK293T cells using stable isotope tracing monitored by mass spectrometry. The extracted-ion chromatograms of the detected $m^{1,6}A$ (MRM: 296.1→164.1, upper panel), D_3-$m^{1,6}A$ (MRM: 299.1→167.1, middle panel), and D_6-$m^{1,6}A$ (MRM: 302.1→170.1, bottom panel) from tRNAs of HEK293T and HeLa cells.

Determination of $m^{1,6}A$ in RNA of mammalian cells

With the synthesized $m^{1,6}A$ standard, we next investigated the potential existence of $m^{1,6}A$ in mammalian RNA by mass spectrometry analysis. The preliminary results showed a peak with a retention time of 3.2 min in the extracted-ion chromatogram (*m/z* 296.1→164.1) from the total RNA of HEK293T cells, which was consistent with the retention time of $m^{1,6}A$ standard (Figure 2A). We added the $m^{1,6}A$ standard to the enzymatically digested nucleosides from total RNA of HEK293T cells. It can be seen that the spiked $m^{1,6}A$ standard had the same retention time as that detected in HEK293T cells and the peak intensities increased with the spiked $m^{1,6}A$ standard (Figure 2A), suggesting that the detected compound should be $m^{1,6}A$. On the contrary, $m^{1,6}A$ was undetectable in the negative control sample of water or the sample with only adding enzymes and omitting RNA (Figure 2A), which excludes the possibility that the detected $m^{1,6}A$ was from the contamination of water or enzymes. We next examined $m^{1,6}A$ in different RNA species from HEK293T cells. The total RNA was separated into mRNA, 28S rRNA, 18S rRNA, 5.8S rRNA, 5S rRNA and tRNAs (Supplementary Figure S7 in Supporting Information), followed by enzymatical digestion and LC–ESI-MS/MS analysis. The results showed that $m^{1,6}A$ mainly existed in tRNAs and was undetectable in other RNA species (Figure 2A).

We further employed high-resolution MS to examine the detected $m^{1,6}A$ from tRNAs of HEK293T cells. The collisional activation the $[M + H]^+$ ions of the $m^{1,6}A$ standard can readily eliminate a ribose moiety to yield the protonated ions of the nucleobase portion (*m/z* 164.0931) as the dominant fragment ions in MS/MS (Supplementary Figure S8 in Supporting Information). Further collisional activation of the ions of *m/z* 164.1 leads to facile loss of C_2H_2N moieties to yield the dominant fragment ions of *m/z* 123.0665 in MS^3 for $m^{1,6}A$ (Supplementary Figure S8 in Supporting Information). The MS/MS and MS^3 analysis showed that the precursor ions and fragment ions (*m/z* shown in blue) of the detected compound in tRNAs of HEK293T cells were identical to their corresponding theoretical values (*m/z* shown in red) as well as to that of the standard (Figure 2B and

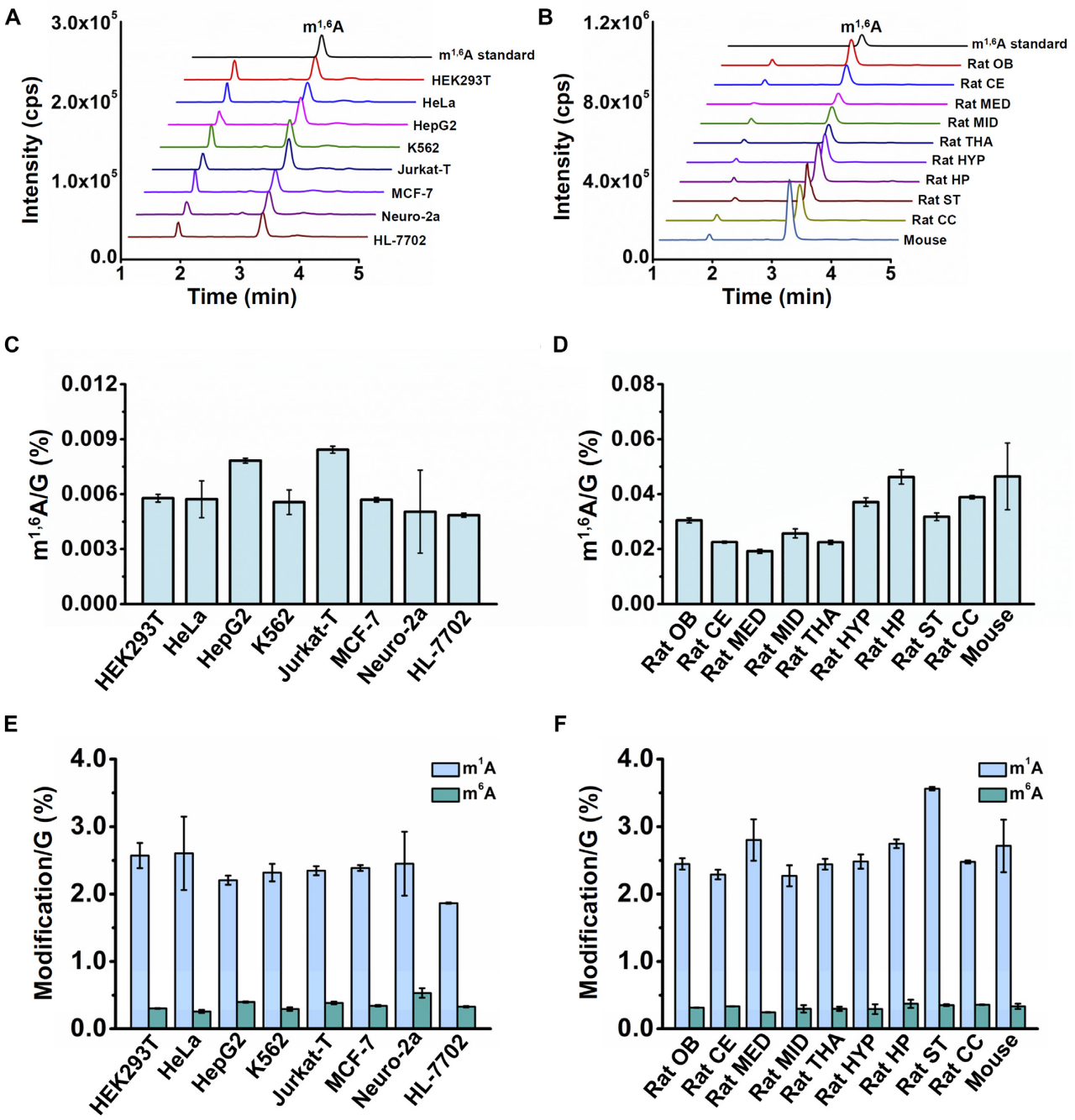

Figure 3. Quantification of $m^{1,6}A$, m^1A and m^6A in tRNAs from different cell lines and tissues. (**A**) The extracted-ion chromatograms of $m^{1,6}A$ from tRNAs of different cell lines. (**B**) The extracted-ion chromatograms of $m^{1,6}A$ from tRNAs of mouse brain tissues and different regions of rat brain tissues. OB: olfactory bulb; CE: cerebellum; MED: medulla; MID: midbrain; THA: thalamus; HYP: hypothalamus; HP: hippocampus: ST: striatum; CC: cerebral cortex. (**C**, **D**) Quantification of $m^{1,6}A$ in tRNAs from different cell lines and tissues. (**E**, **F**) Quantification of m^1A and m^6A in tRNAs from different cell lines and tissues.

C), further confirming the detected $m^{1,6}A$ in tRNAs. Collectively, the results demonstrate that $m^{1,6}A$ is present in tRNAs of HEK293T cells.

Metabolic labeling of $m^{1,6}A$

We further carried out the stable isotope tracing monitored by mass spectrometry assay to evaluate the methyl group donor for $m^{1,6}A$. It has been well known that L-methionine (Met) could be converted into *S*-adenosyl-L-methionine (SAM) by methionine adenosyltransferase and SAM is a methyl group donor for many methylated nucleosides (31). If $m^{1,6}A$ exists in mammalian cells, culturing cells in the DMEM medium supplied with isotopically labeled L-methionine (D_3-Met) should lead to the transfer of the CD_3 group from D_3-SAM to $m^{1,6}A$. Theoretically, single

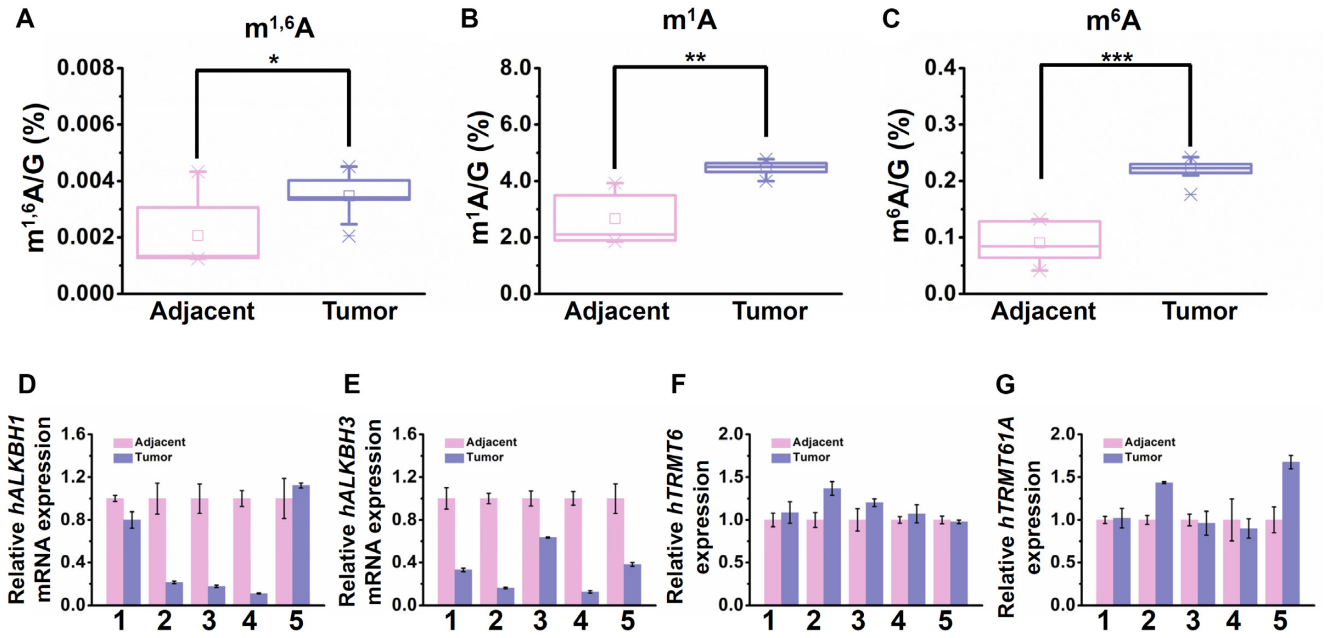

Figure 4. Quantification of RNA adenosine modifications in tRNAs and the mRNA levels of *hALKBH1*, *hALKBH3*, *hTRMT6* and *hTRMT61A* in human breast cancer tissues and tumor-adjacent normal tissues. (**A**–**C**) Quantification and statistical analysis of $m^{1,6}A$, m^1A and m^6A in tRNAs. (**D**–**G**) The relative mRNA levels of *hALKBH1*, *hALKBH3*, *hTRMT6* and *hTRMT61A*. Triplicate measurements were carried out. A total of 10 tissues from five breast cancer patients were analyzed.

and dual CD_3 might be added to $m^{1,6}A$, including D_3-$m^{1,6}A$ (CD_3-labeled N1 or N6) and D_6-$m^{1,6}A$ (CD_3-labeled both N1 and N6). The results showed that, as expected, $m^{1,6}A$, D_3-$m^{1,6}A$ and D_6-$m^{1,6}A$, were clearly detected in tRNAs of HEK293T and HeLa cells (Figure 2D and E). The concentration of D_3-Met in the medium is 60% of the total methionine (D_3-Met/ (D_3-Met + Met)). Quantification data showed that approximately 60% of the measured $m^{1,6}A$ carried CD_3 group, which is comparable to the theoretical percentage of D_3-Met in total methionine in the medium. Collectively, the results further confirm the presence of $m^{1,6}A$ in tRNAs of mammalian cells and SAM is the methyl donor for $m^{1,6}A$.

Quantification of $m^{1,6}A$ in tRNAs of multiple cell lines and tissues

With the discovery of $m^{1,6}A$ in tRNAs of HEK293T and HeLa cells, we next examined whether $m^{1,6}A$ is a prevalent modification present in tRNAs of mammals. In this respect, the tRNAs from a variety of mammalian cells, including HepG2 cells, K562 cells, Jurkat-T cells, MCF-7 cells, HL-7702 cells, and mouse Neuro-2a cells, were extracted and analyzed. The results showed that $m^{1,6}A$ could be detected in all these cell lines (Figure 3A). Furthermore, $m^{1,6}A$ was present in tRNAs of rat and mouse brain tissues (Figure 3B). Notably, $m^{1,6}A$ was detected in all the different regions of rat brain tissues (Figure 3B). The measured $m^{1,6}A$ ranged from 0.0049% to 0.0084% and from 0.019% to 0.047% in tRNAs of mammalian cells and tissues, respectively (Figure 3C and D). Obviously, the level of $m^{1,6}A$ is low than that of m^1A and m^6A in tRNAs of mammals (Figure 3E and F).

It has been reported that RNA modifications are involved in a variety of human diseases (32). Herein, we further evaluated whether there is a difference in the level of $m^{1,6}A$ between human breast cancer tissues and tumor-adjacent normal tissues. The statistical results showed that the levels of $m^{1,6}A$, m^1A and m^6A in tRNAs significantly increased in human breast cancer tissues compared to tumor-adjacent normal tissues (Figure 4A–C). We further examined the expression of *hALKBH1* and *hALKBH3* in these tissues since ALKBH1 can demethylate m^1A and ALKBH3 can demethylate both m^1A and m^6A (33–35). The results showed that the mRNA levels of *hALKBH1* and *hALKBH3* were generally decreased in human breast cancer tissues (Figure 4D and E), revealing that the decreased expressions of *hALKBH1* and *hALKBH3* in human breast cancer tissues are correlated to the increased levels of $m^{1,6}A$, m^1A and m^6A in tRNAs. Moreover, m^1A at position 58 (m^1A_{58}) of human cytoplasmic tRNAs was catalyzed by TRMT6/61A methyltransferase (36). However, the mRNA levels of *hTRMT6* and *hTRMT61A* were only slightly increased in human breast cancer tissues (Figure 4F and G). Taken together, these results indicate that the increased contents of $m^{1,6}A$, m^1A and m^6A in tRNAs of human breast cancer tissues are closely correlated to the expression of *hALKBH1* and *hALKBH3*.

Determination of the site of $m^{1,6}A$ in m^1A_{58}-containing tRNAs

m^1A in tRNAs is a highly conserved modification in mammalian cells. TRMT6/61A methyltransferase complex is responsible for forming m^1A_{58} in tRNAs (36). The crystal structure of TRMT6/61A bound to tRNAs displayed that

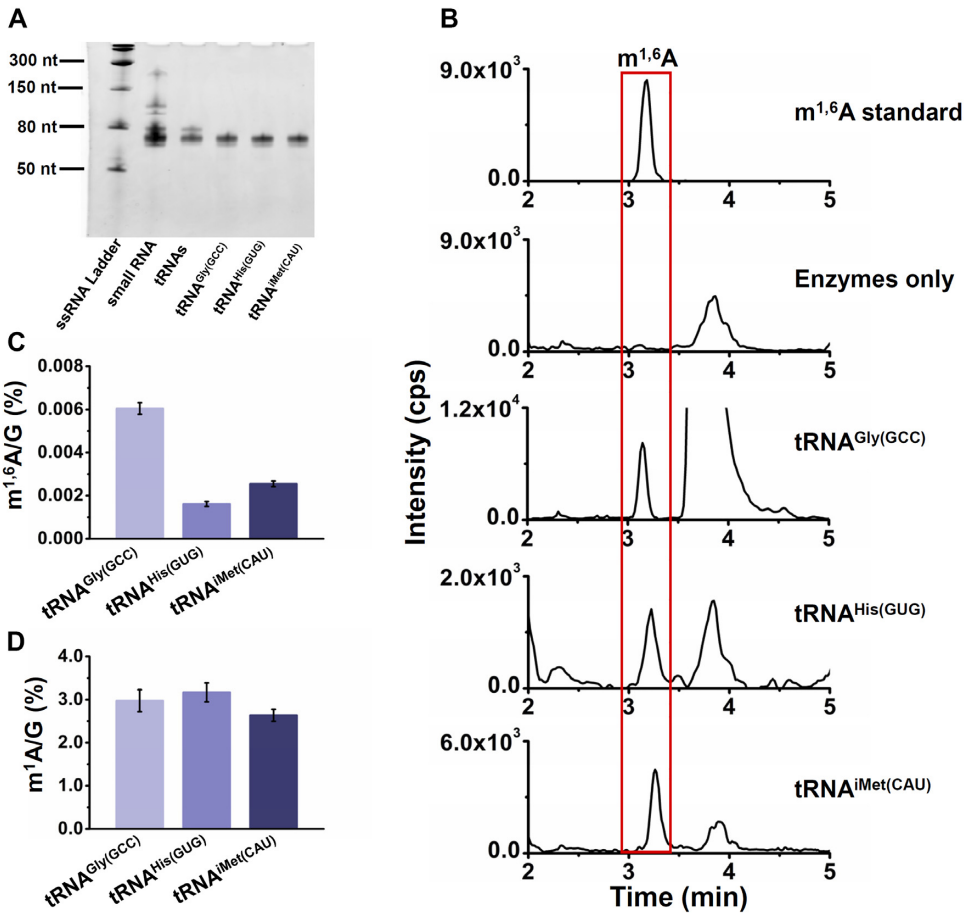

Figure 5. Identification and quantification of $m^{1,6}A$ in individual tRNA from HEK293T cells. (**A**) Urea–PAGE analysis of isolated small RNA (<200 nt), tRNAs, $tRNA^{Gly(GCC)}$, $tRNA^{His(GUG)}$ and $tRNA^{iMet(CAU)}$ from HEK293T cells. (**B**) The extracted-ion chromatograms of $m^{1,6}A$ from $tRNA^{Gly(GCC)}$, $tRNA^{His(GUG)}$ and $tRNA^{iMet(CAU)}$. (**C**, **D**) Quantification of $m^{1,6}A$ and m^1A in individual tRNA from HEK293T cells.

the methyltransferase complex was highly conserved to the secondary structure of the substrate tRNAs (37). Thus, we suspect that the biosynthesis of $m^{1,6}A$ may be through the further methylation of m^1A at the N6 position, resulting the generation of $m^{1,6}A$ at position 58 of tRNAs. To verify our hypothesis, we purified three m^1A_{58}-containing tRNAs, including $tRNA^{Gly(GCC)}$, $tRNA^{His(GUG)}$ and $tRNA^{iMet(CAU)}$ (Figure 5A). These purified tRNAs were enzymatically digested and analyzed by LC–ESI-MS/MS. The results demonstrated that all these tRNAs carried $m^{1,6}A$ (Figure 5B). The quantification data showed that the levels of $m^{1,6}A$ and m^1A ranged from 0.0016% to 0.0060% and from 2.6% to 3.2% in these individual tRNA, respectively (Figure 5C and D).

We next examined whether $m^{1,6}A$ is located at position 58 of tRNAs. To this end, we developed a strategy of DNA hybridization protection combined with S1 nuclease digestion. In this strategy, a 22-mer biotin-labeled DNA probe complementary to $tRNA^{Gly(GCC)}$ was used to hybridize to the region that contains m^1A_{58}, followed by S1 nuclease digestion (Figure 6A and B). S1 nuclease could specifically digest the single-stranded RNA, but not the hybrid of RNA/DNA duplex region. Therefore, the remaining 22-bp RNA/DNA hybrid was recovered by PuriMag G-Streptavidin magnetic beads after S1 nuclease digestion (Figure 6A and B). The gel electrophoresis analysis confirmed the successfully isolated 22-bp fragment (Figure 6C). LC–ESI-MS/MS analysis of the 22-bp fragment demonstrated that the 22-nt fragment from $tRNA^{Gly(GCC)}$ contained $m^{1,6}A$ (Figure 6D), with the level being 0.022% (Supplementary Figure S9 in Supporting Information). Because the 22-nt fragment in $tRNA^{Gly(GCC)}$ contains only one adenosine at position 58 (Figure 6A), the detected $m^{1,6}A$ theoretically is from the position 58 of $tRNA^{Gly(GCC)}$. In addition, we also synthesized shorter 20-mer and 18-mer DNA probe to carry out the DNA hybridization protection combined with S1 nuclease digestion assay. The LC–ESI-MS/MS analysis showed that similar results were obtained with using different length of DNA probes (Supplementary Figure S10 and Supplementary Figure S11 in Supporting Information). Collectively, these results with using different length of DNA probes (22-mer, 20-mer and 18-mer) reveal that $m^{1,6}A$ exists at position 58 of $tRNA^{Gly(GCC)}$. Here, we focused on the study of $m^{1,6}A$ in m^1A_{58}-containing $tRNA^{Gly(GCC)}$. The other m^1A_{58}-containing tRNAs may also carry $m^{1,6}A$ at position 58, which can be explored in future studies.

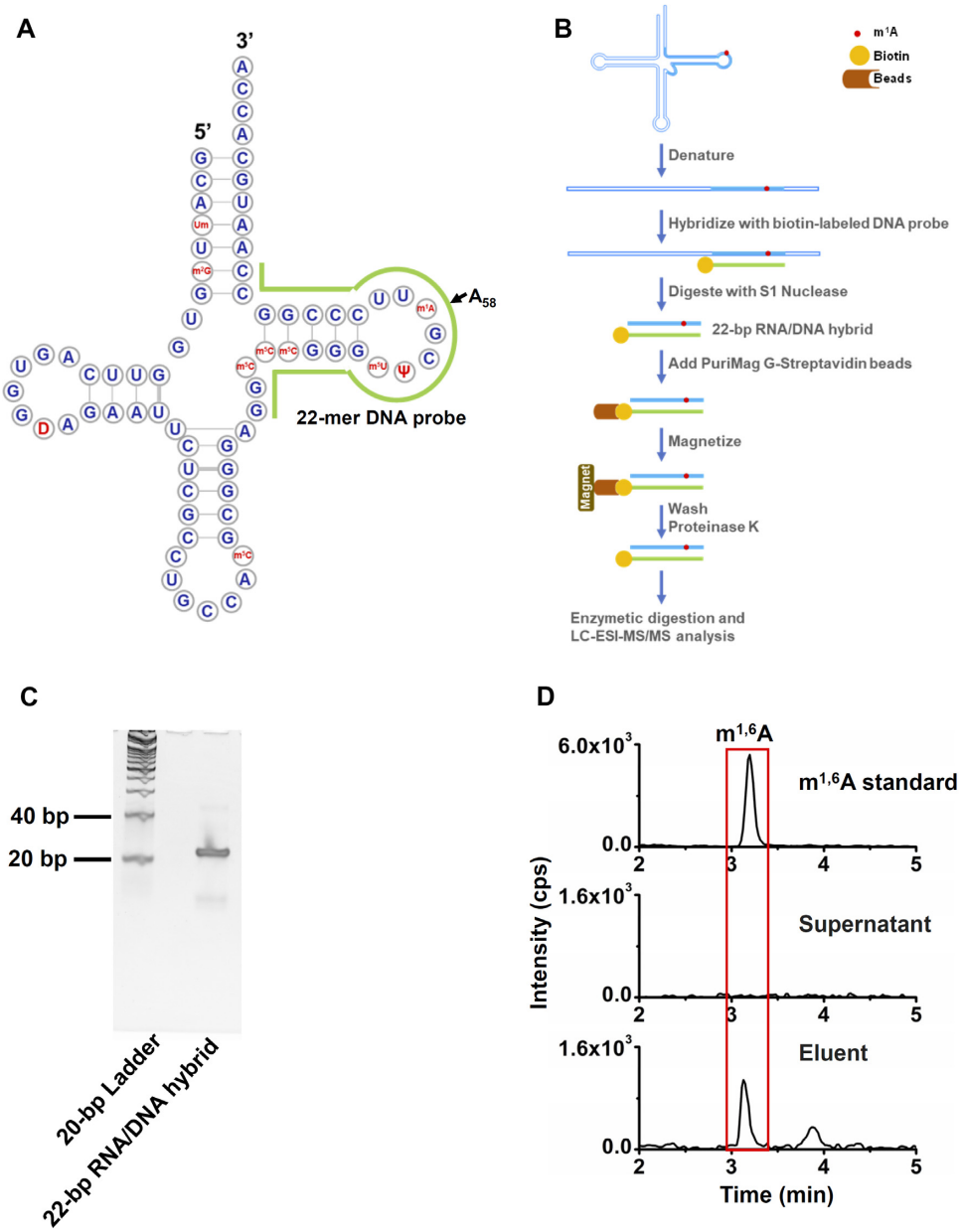

Figure 6. Determination of the site of $m^{1,6}A$ in $tRNA^{Gly(GCC)}$ from HEK293T cells. (**A**) The sequence and modifications of $tRNA^{Gly(GCC)}$. Shown in red represents different RNA modifications. The green line represents the DNA probe complementary to the 22-nt fragment region. (**B**) Schematic illustration of the purification of the 22-nt fragment region that contains m^1A_{58}. (**C**) PAGE analysis of the 22-bp RNA/DNA hybrid. (**D**) The extracted-ion chromatograms of $m^{1,6}A$ from $m^{1,6}A$ standard (upper panel), supernatant (middle panel), and eluent (bottom panel) by LC-ESI-MS/MS analysis.

TRMT6/61A catalyzes the formation of $m^{1,6}A$ in tRNAs

We next explored the potential methyltransferase responsible for the formation of $m^{1,6}A$ in tRNAs. The biosynthesis of $m^{1,6}A$ may be through the further methylation of m^1A at the N6 position or methylation of m^6A at the N1 position to form $m^{1,6}A$. As for the further methylation of m^1A at the N6 position, m^1A_{58} in tRNAs is located in the TΨC loop with a GUUCRA (R = A/G) motif (20), thus the methyltransferase of $m^{1,6}A$ should recognize such motif and secondary structure of tRNAs. Among the reported m^6A methyltransferases, the METTL3/METTL14 complex (38,39), METTL5/TRMT112 complex (40) and ZCCHC4 (15) all exhibit strong substrate specificity and are unlikely to exert further methylation of m^1A_{58} at the N6 position in tRNAs.

It has been reported that the methyltransferase METTL16 can methylate adenosine to form m^6A in pre-mRNAs, U6 snRNA and other highly structured lncRNAs (41). METTL16 shows no obvious recognition motif and could recognize substrates with secondary structures, making it a potential candidate for $m^{1,6}A$ methyltransferase. We therefore expressed and purified recombinant hMTD16 protein that had similar activity as hMETTL16

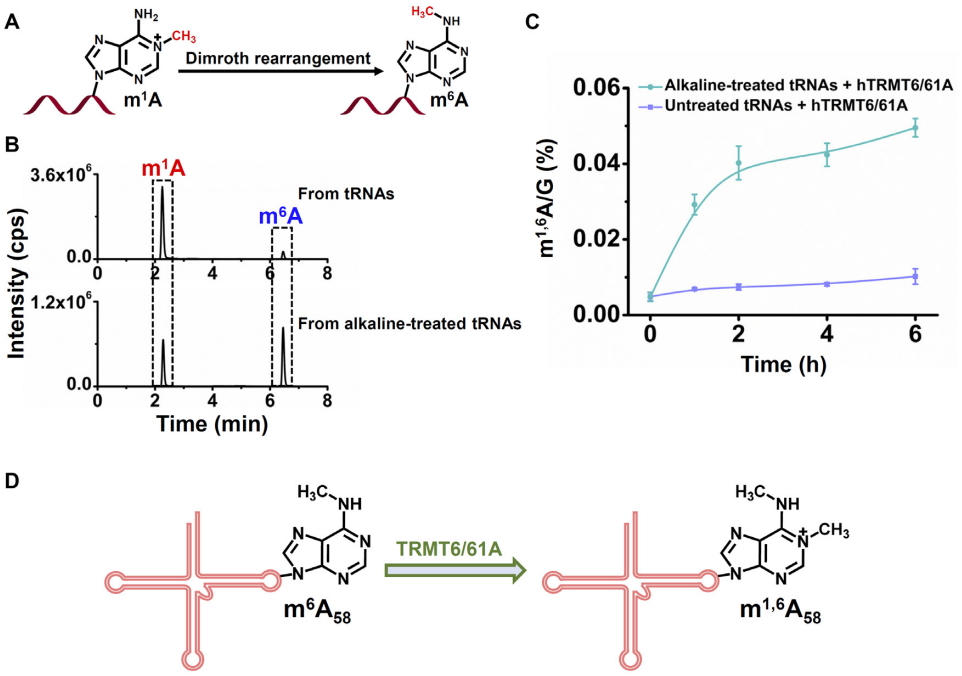

Figure 7. hTRMT6/61A catalyzes the further methylation of m^6A_{58} at the N1 position to form $m^{1,6}A_{58}$ in tRNAs. (**A**) Schematic illustration of m^1A-to-m^6A rearrangement (Dimroth rearrangement). (**B**) The extracted-ion chromatograms of m^1A and m^6A in untreated tRNAs (upper panel) and alkaline-treated tRNAs (bottom panel). (**C**) Quantification of $m^{1,6}A$ in alkaline-treated tRNAs and untreated tRNAs after incubation with hTRMT6/61A at different times. (**D**) Schematic illustration showing that TRMT6/61A catalyzes the methylation of m^6A_{58} at the N1 position to form $m^{1,6}A_{58}$ in tRNAs.

protein (42,43) (Supplementary Figure S12A in Supporting Information). The activity of hMTD16 was verified using a synthetic hairpin RNA bearing the hMTD16 recognition site (ACAGA) (Supplementary Figure S12B in Supporting Information). Incubation of the hairpin RNA with hMTD16 led to formation of m^6A (Supplementary Figure S12C in Supporting Information), suggesting the recombinant hMTD16 exhibits m^6A methyltransferase activity. However, incubation of the tRNAs from HEK293T cells with hMTD16 in the presence of SAM didn't lead to the obvious increase of $m^{1,6}A$ or m^6A (Supplementary Figure S12D and Supplementary Figure S13 in Supporting Information). We also synthesized and utilized D_3-SAM as the methyl group donor in the methylation assay (Supplementary Figure S12E and Supplementary Figure S14 in Supporting Information). Likewise, no D_3-$m^{1,6}A$ was detected (Supplementary Figure S12F in Supporting Information), indicating that METTL16 is not responsible for the formation of $m^{1,6}A$ in tRNAs.

The DNA hybridization protection combined with S1 nuclease digestion assay indicated that m^6A was also present at position 58 of $tRNA^{Gly(GCC)}$ (Supplementary Figure S15 in Supporting Information). Thus, it is possible that the biosynthesis of $m^{1,6}A$ may be through the further methylation of m^6A at the N1 position to form $m^{1,6}A$. It has been reported that TRMT10 is responsible for the methylation of purine at position 9 in some tRNAs (17,44), and TRMT6/61A is responsible for the deposition of m^1A at position 58 in tRNAs (36,45). Since $m^{1,6}A$ is located at position 58 of tRNAs, we next explored the formation of $m^{1,6}A$ by TRMT6/61A protein complex. We expressed and purified the recombinant hTRMT6/61A protein complex (Supplementary Figure S16 in Supporting Information). Incubation of the hALKBH3-treated tRNAs with hTRMT6/61A led to a dramatic increase of m^1A (Supplementary Figure S17 in Supporting Information), confirming the purified recombinant hTRMT6/61A protein complex has good activity.

We carried out the *in vitro* methylation assay to examine whether TRMT6/61A can methylate m^6A to form $m^{1,6}A$ in tRNAs. First, the isolated tRNAs were subjected to alkaline treatment (pH 9.0) at 50°C for 1 h to allow the Dimroth rearrangement (m^1A-to-m^6A rearrangement) according to previously described method (21) (Figure 7A). It can be seen that the level of m^6A was increased after alkaline treatment (Figure 7B and Supplementary Figure S18 in Supporting Information). The alkaline-treated tRNAs were purified and then further incubated with hTRMT6/61A. The result showed a time-dependent increase of $m^{1,6}A$ (Figure 7C), suggesting that TRMT6/61A can further methylate m^6A at the N1 position to form $m^{1,6}A$ in tRNAs. In addition, we also carried out the incubation of untreated tRNAs (without alkaline treatment) with hTRMT6/61A. Again, we observed an increased level of $m^{1,6}A$ (Figure 7C). Since the level of m^6A in alkaline-treated tRNAs was much higher than that in tRNAs without alkaline treatment, the formed $m^{1,6}A$ upon incubation with hTRMT6/61A from alkaline-treated tRNAs was therefore much higher than that from tRNAs without alkaline treatment (Figure 7C). Taken together, these results suggest that TRMT6/61A is responsible for the formation of $m^{1,6}A$ in tRNAs. We speculate that a small fraction of m^1A_{58} will be rearranged to m^6A_{58} *in vivo*

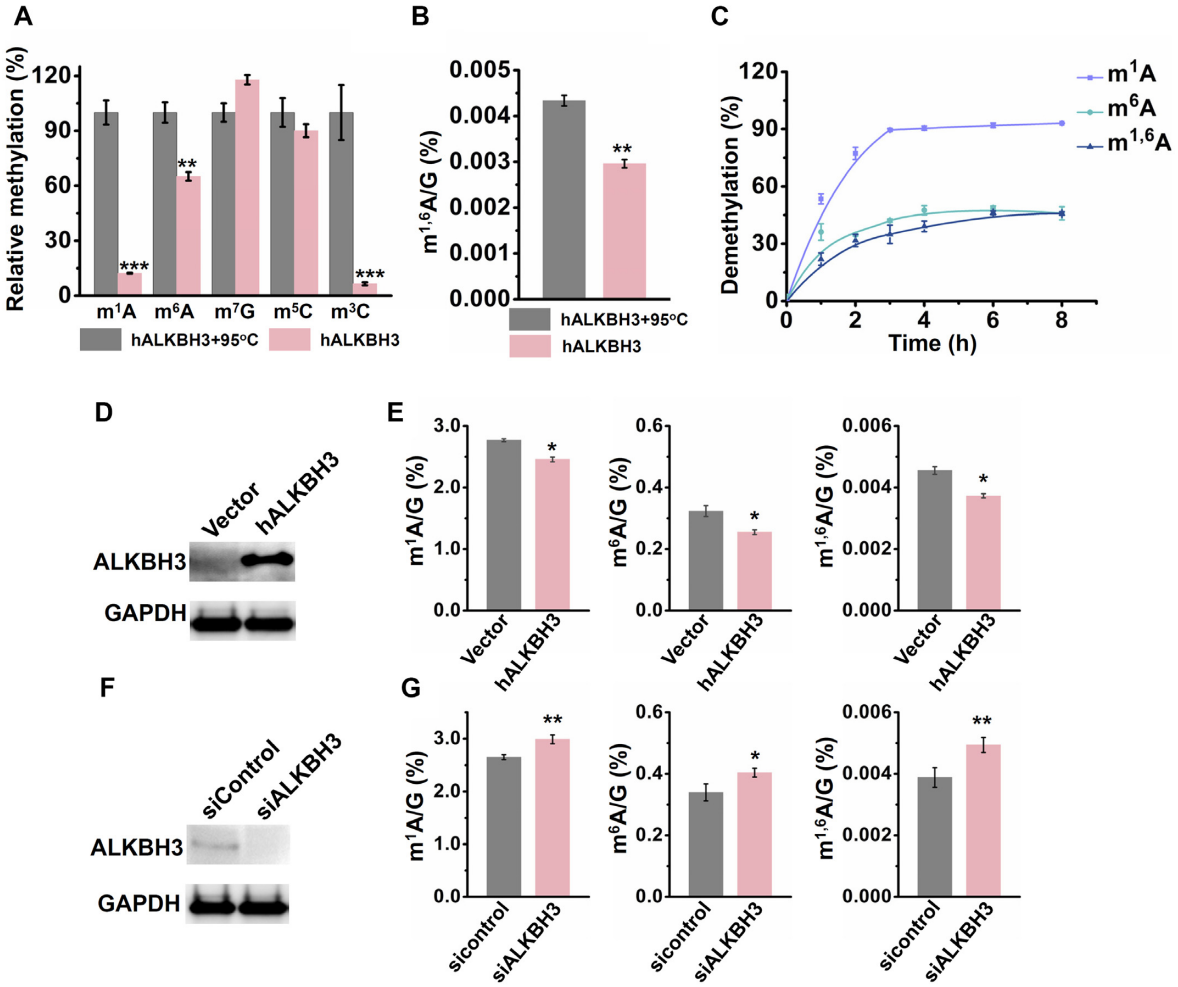

Figure 8. hALKBH3 catalyzes the demethylation of $m^{1,6}A$ in tRNAs. (**A**, **B**) Change of the levels of m^1A, m^6A, m^7G, m^5C, m^3C, and $m^{1,6}A$ in tRNAs of HEK293T cells after hALKBH3 or heat-inactivated hALKBH3 treatment. (**C**) Demethylation of m^1A, m^6A and $m^{1,6}A$ in tRNAs at different time upon hALKBH3 treatment. (**D**) Western blotting of hALKBH3 upon overexpression. (**E**) Measured levels of m^1A, m^6A and $m^{1,6}A$ in tRNAs of HEK293T cells upon overexpression of *hALKBH3*. (**F**) Western blotting of hALKBH3 upon siRNA knockdown. (**G**) Measured levels of m^1A, m^6A and $m^{1,6}A$ in tRNAs of HEK293T cells upon knockdown of *hALKBH3*. Data were presented as means ± SD from three independent experiments. * $P < 0.05$, ** $P < 0.01$, *** $P < 0.001$.

(although so far no methyltransferase has been reported for m^6A in tRNAs, we cannot exclude the possibility that m^6A_{58} is deposited by certain methyltransferase), and the generated m^6A_{58} will be further methylated to form $m^{1,6}A_{58}$ by TRMT6/61A (Figure 7D).

ALKBH3 catalyzes the demethylation of $m^{1,6}A$ in tRNAs

m^1A_{58} in tRNAs can be demethylated by ALKBH1 and ALKBH3 (29,33,46). According to the finding that the levels of $m^{1,6}A$ and m^1A in tRNAs of human breast cancer tissues are correlated to the expression of *hALKBH1* and *hALKBH3* (Figure 4), we thus speculate that these demethylases for m^1A_{58} may also potentially demethylate $m^{1,6}A$. Along this line, we expressed and purified recombinant hALKBH3 protein (Supplementary Figure S19A in Supporting Information), and carried out the *in vitro* demethylation assay. Incubation of the tRNAs from HEK293T cells with hALKBH3 led to a dramatic decrease of m^1A, m^6A, m^3C and $m^{1,6}A$, but not the levels of m^7G or m^5C (Figure 8A and B). The results suggested that hALKBH3 had demethylation activity toward $m^{1,6}A$. Additionally, hALKBH3 exhibited stronger demethylation activity toward m^1A than m^6A and $m^{1,6}A$ (Figure 8C). The observed demethylation activity of hALKBH3 toward m^1A, m^6A and m^3C in tRNAs is also consistent with previous reports (29,46). In addition to the *in vitro* assay, the overexpression of *hALKBH3* in HEK293T cells caused marked decline in the level of m^1A, m^6A and $m^{1,6}A$ (Figure 8D and E). Reciprocally, knockdown of *hALKBH3* by siRNA in HEK293T cells induced a significant increase of the levels of m^1A, m^6A and $m^{1,6}A$ (Figure 8F and G). Similar phenomena were observed by using mALKBH3 (Supplementary Figure S19B and S20 in Supporting Information). Taken together, these results suggest that ALKBH3 is responsible for the demethylation of $m^{1,6}A$ in tRNAs.

In addition, we also expressed and purified recombinant hALKBH1 protein (Supplementary Figure S21A in Supporting Information) and carried out the *in vitro* demethylation assay. As expected, incubation of tRNAs

with hALKBH1 led to a significant decrease in the m^1A level (Supplementary Figure S21B in Supporting Information). However, m^6A, m^7G, and $m^{1,6}A$ in tRNAs did not change significantly (Supplementary Figure S21B and S21C in Supporting Information), indicating that ALKBH1 is only capable of demethylating m^1A in tRNAs and cannot demethylate $m^{1,6}A$ in tRNAs. Similarly, *in vivo* overexpression and knockdown of *hALKBH1* indeed resulted in the corresponding change of m^1A in tRNAs (Supplementary Figure S21D–G in Supporting Information), but no noticeable difference was observed for $m^{1,6}A$ in tRNAs (Supplementary Figure S21E and S21G in Supporting Information). In addition, we used hALKBH1 to treat the single $tRNA^{iMet}$ that was confirmed to carry $m^{1,6}A$. The result also showed that hALKBH1 could demethylate m^1A in $tRNA^{iMet}$ but not $m^{1,6}A$ (Supplementary Figure S22 in Supporting Information). These results show that ALKBH1 is unlikely the demethylases for $m^{1,6}A$ in tRNAs.

Intriguingly, some RNA modifications formed by physiologically enzymatic processes could also be generated by damaging agents, thus blurring the line between a physiological mark and a damage-induced modification (i.e. RNA lesion) (47). For example, m^1A and 3-methylcytosine (m^3C) could be produced by RNA methyltransferases or by damaging agents (23,48,49). In this point, $m^{1,6}A$ might also be considered as an RNA lesion since its formation is involved in the nonenzymatic rearrangement. In addition, LC–ESI-MS/MS with MRM detection mode generally could offer the detection sensitivity of nucleosides at femtomole level (50–52), allowing the detection of low-abundant RNA lesions produced by endogenous or exogenous damaging agents. Repair of RNA lesion is critical because some RNA lesions have the potential to disturb posttranscriptional events (53). Clearly, $m^{1,6}A_{58}$ could be demethylated (or repaired) by ALKBH3 to restore to unmodified adenosine. We observed a higher level of $m^{1,6}A$ in breast cancer tissues, which could be attributed to the lower expression level of ALKBH3 in breast cancer tissues. Although $m^{1,6}A$ could be viewed as an RNA lesion, it is possible that it may also play potentially regulatory role like 8-oxoguanine in DNA and RNA (54,55). We anticipate that future investigations will provide us further understanding of $m^{1,6}A$.

In summary, with the synthesized standard, we identified $m^{1,6}A$ in tRNAs of mammals. We confirmed that $m^{1,6}A$ is located at position 58 of tRNAs and is prevalent in mammalian cells and tissues. $m^{1,6}A$ could be formed from the further methylation of m^6A at the N1 position by TRMT6/61A. We demonstrated that ALKBH3 could demethylate $m^{1,6}A$ in tRNAs. Based the obtained results together previous studies, we proposed a pathway for the dynamic regulation of the adenosine methylation at position 58 in tRNAs (Supplementary Figure S23 in Supporting Information). The methyltransferase complex TRMT6/61A could methylate adenosine at position 58 of tRNAs to form m^1A_{58}. m^1A_{58} could be demethylated by ALKBH1 and ALKBH3 to restore adenosine. On the other hand, m^6A_{58} that may be from the rearrangement of m^1A_{58} (or formed by certain methyltransferase) could be further methylated at the N1 position to form $m^{1,6}A_{58}$ by TRMT6/61A. The generated $m^{1,6}A_{58}$ could be demethylated by ALKBH3. The significantly increased level of $m^{1,6}A$ in human breast cancer tissues indicates it may be correlated with cancer development. Taken together, we identified a modification of $m^{1,6}A$ that has not been reported in living organisms before, which diversifies RNA modifications and may indicate a new regulation mechanism for tRNA modification-mediated gene expression.

SUPPLEMENTARY DATA

Supplementary Data are available at NAR Online.

ACKNOWLEDGEMENTS

We thank Dr Wen-Bo Liu and Dr Qiang-Hui Zhou (Wuhan University, PR China) for the helpful discussion on interpreting NMR spectra.

FUNDING

National Natural Science Foundation of China [22277093, 22074110, 21721005]. Funding for open access charge: National Natural Science Foundation of China.
Conflict of Interest statement. None declared.

REFERENCES

1. Chen,K., Zhao,B.S. and He,C. (2016) Nucleic acid modifications in regulation of gene expression. *Cell Chem. Biol.*, **23**, 74–85.
2. Chen,Y., Hong,T., Wang,S., Mo,J., Tian,T. and Zhou,X. (2017) Epigenetic modification of nucleic acids: from basic studies to medical applications. *Chem. Soc. Rev.*, **46**, 2844–2872.
3. Boccaletto,P., Stefaniak,F., Ray,A., Cappannini,A., Mukherjee,S., Purta,E., Kurkowska,M., Shirvanizadeh,N., Destefanis,E., Groza,P. *et al.* (2022) MODOMICS: a database of RNA modification pathways. 2021 update. *Nucleic Acids Res.*, **50**, D231–D235.
4. Roundtree,I.A., Evans,M.E., Pan,T. and He,C. (2017) Dynamic RNA modifications in gene expression regulation. *Cell*, **169**, 1187–1200.
5. Fu,L., Guerrero,C.R., Zhong,N., Amato,N.J., Liu,Y., Liu,S., Cai,Q., Ji,D., Jin,S.G., Niedernhofer,L.J. *et al.* (2014) Tet-mediated formation of 5-hydroxymethylcytosine in RNA. *J. Am. Chem. Soc.*, **136**, 11582–11585.
6. Chen,M.Y., Qi,C.B., Tang,X.M., Ding,J.H., Yuan,B.F. and Feng,Y.Q. (2022) Comprehensive profiling and evaluation of the alteration of RNA modifications in thyroid carcinoma by liquid chromatography-tandem mass spectrometry. *Chin. Chem. Lett.*, **33**, 3772–3776.
7. Frye,M., Harada,B.T., Behm,M. and He,C. (2018) RNA modifications modulate gene expression during development. *Science*, **361**, 1346–1349.
8. Wiener,D. and Schwartz,S. (2021) The epitranscriptome beyond m(6)A. *Nat. Rev. Genet.*, **22**, 119–131.
9. He,P.C. and He,C. (2021) m(6) a RNA methylation: from mechanisms to therapeutic potential. *EMBO J.*, **40**, e105977.
10. Batista,P.J., Molinie,B., Wang,J., Qu,K., Zhang,J., Li,L., Bouley,D.M., Lujan,E., Haddad,B., Daneshvar,K. *et al.* (2014) m(6)A RNA modification controls cell fate transition in mammalian embryonic stem cells. *Cell Stem Cell*, **15**, 707–719.
11. Xiang,Y., Laurent,B., Hsu,C.H., Nachtergaele,S., Lu,Z., Sheng,W., Xu,C., Chen,H., Ouyang,J., Wang,S. *et al.* (2017) RNA m6A methylation regulates the ultraviolet-induced DNA damage response. *Nature*, **543**, 573–576.
12. Chen,M.Y., Gui,Z., Chen,K.K., Ding,J.H., He,J.G., Xiong,J., Li,J.L., Wang,J., Yuan,B.F. and Feng,Y.Q. (2022) Adolescent alcohol exposure alters DNA and RNA modifications in peripheral blood by

liquid chromatography-tandem mass spectrometry analysis. *Chin. Chem. Lett.*, **33**, 2086–2090.
13. Huang,H.L., Weng,H.Y., Deng,X.L. and Chen,J.J. (2020) RNA modifications in cancer: functions, mechanisms, and therapeutic implications. *Annu. Rev. Cancer Biol.*, **4**, 221–240.
14. Wang,X., Lu,Z., Gomez,A., Hon,G.C., Yue,Y., Han,D., Fu,Y., Parisien,M., Dai,Q., Jia,G. *et al.* (2014) N6-methyladenosine-dependent regulation of messenger RNA stability. *Nature*, **505**, 117–120.
15. Ma,H., Wang,X., Cai,J., Dai,Q., Natchiar,S.K., Lv,R., Chen,K., Lu,Z., Chen,H., Shi,Y.G. *et al.* (2019) N(6-)Methyladenosine methyltransferase ZCCHC4 mediates ribosomal RNA methylation. *Nat. Chem. Biol.*, **15**, 88–94.
16. Alarcon,C.R., Lee,H., Goodarzi,H., Halberg,N. and Tavazoie,S.F. (2015) N6-methyladenosine marks primary microRNAs for processing. *Nature*, **519**, 482–485.
17. Vilardo,E., Amman,F., Toth,U., Kotter,A., Helm,M. and Rossmanith,W. (2020) Functional characterization of the human tRNA methyltransferases TRMT10A and TRMT10B. *Nucleic Acids Res.*, **48**, 6157–6169.
18. Sergiev,P.V., Aleksashin,N.A., Chugunova,A.A., Polikanov,Y.S. and Dontsova,O.A. (2018) Structural and evolutionary insights into ribosomal RNA methylation. *Nat. Chem. Biol.*, **14**, 226–235.
19. Suzuki,T., Yashiro,Y., Kikuchi,I., Ishigami,Y., Saito,H., Matsuzawa,I., Okada,S., Mito,M., Iwasaki,S., Ma,D. *et al.* (2020) Complete chemical structures of human mitochondrial tRNAs. *Nat. Commun.*, **11**, 4269.
20. Li,X., Xiong,X., Zhang,M., Wang,K., Chen,Y., Zhou,J., Mao,Y., Lv,J., Yi,D., Chen,X.W. *et al.* (2017) Base-Resolution mapping reveals distinct m(1)A methylome in Nuclear- and Mitochondrial-Encoded transcripts. *Mol. Cell*, **68**, 993–1005.
21. Dominissini,D., Nachtergaele,S., Moshitch-Moshkovitz,S., Peer,E., Kol,N., Ben-Haim,M.S., Dai,Q., Di Segni,A., Salmon-Divon,M., Clark,W.C. *et al.* (2016) The dynamic N(1)-methyladenosine methylome in eukaryotic messenger RNA. *Nature*, **530**, 441–446.
22. Li,X., Xiong,X., Wang,K., Wang,L., Shu,X., Ma,S. and Yi,C. (2016) Transcriptome-wide mapping reveals reversible and dynamic N(1)-methyladenosine methylome. *Nat. Chem. Biol.*, **12**, 311–316.
23. Xiong,X., Li,X. and Yi,C. (2018) N(1)-methyladenosine methylome in messenger RNA and non-coding RNA. *Curr. Opin. Chem. Biol.*, **45**, 179–186.
24. Zorbas,C., Nicolas,E., Wacheul,L., Huvelle,E., Heurgue-Hamard,V. and Lafontaine,D.L. (2015) The human 18S rRNA base methyltransferases DIMT1L and WBSCR22-TRMT112 but not rRNA modification are required for ribosome biogenesis. *Mol. Biol. Cell*, **26**, 2080–2095.
25. Sloan,K.E., Warda,A.S., Sharma,S., Entian,K.D., Lafontaine,D.L. and Bohnsack,M.T. (2016) Tuning the ribosome: the influence of rRNA modification on eukaryotic ribosome biogenesis and function. *RNA Biol.*, **14**, 1138–1152.
26. Lan,M.D., Xiong,J., You,X.J., Weng,X.C., Zhou,X., Yuan,B.F. and Feng,Y.Q. (2018) Existence of diverse modifications in Small-RNA species composed of 16-28 nucleotides. *Chem.-Eur. J.*, **24**, 9949–9956.
27. You,X.J., Liu,T., Ma,C.J., Qi,C.B., Tong,Y., Zhao,X., Yuan,B.F. and Feng,Y.Q. (2019) Determination of RNA hydroxylmethylation in mammals by mass spectrometry analysis. *Anal. Chem.*, **91**, 10477–10483.
28. Doxtader,K.A., Wang,P., Scarborough,A.M., Seo,D., Conrad,N.K. and Nam,Y. (2018) Structural basis for regulation of METTL16, an S-Adenosylmethionine homeostasis factor. *Mol. Cell*, **71**, 1001–1011.
29. Chen,Z., Qi,M., Shen,B., Luo,G., Wu,Y., Li,J., Lu,Z., Zheng,Z., Dai,Q. and Wang,H. (2019) Transfer RNA demethylase ALKBH3 promotes cancer progression via induction of tRNA-derived small RNAs. *Nucleic Acids Res.*, **47**, 2533–2545.
30. Bredereck,H., Haas,H. and Martini,A. (1948) Uber methylierte nucleoside und purine und ihre pharmakologischenWir kungen, 11. Mitteil.: methylierung vonNucleosiden durch I)imethylsulfat. *Chem. Ber.*, **81**, 307–313.
31. Landgraf,B.J., McCarthy,E.L. and Booker,S.J. (2016) Radical S-Adenosylmethionine enzymes in human health and disease. *Annu. Rev. Biochem.*, **85**, 485–514.
32. Barbieri,I. and Kouzarides,T. (2020) Role of RNA modifications in cancer. *Nat. Rev. Cancer*, **20**, 303–322.
33. Liu,F., Clark,W., Luo,G., Wang,X., Fu,Y., Wei,J., Wang,X., Hao,Z., Dai,Q., Zheng,G. *et al.* (2016) ALKBH1-Mediated tRNA demethylation regulates translation. *Cell*, **167**, 816–828.
34. Ueda,Y., Ooshio,I., Fusamae,Y., Kitae,K., Kawaguchi,M., Jingushi,K., Hase,H., Harada,K., Hirata,K. and Tsujikawa,K. (2017) AlkB homolog 3-mediated tRNA demethylation promotes protein synthesis in cancer cells. *Sci. Rep.*, **7**, 42271.
35. Chen,Z., Qi,M., Shen,B., Luo,G., Wu,Y., Li,J., Lu,Z., Zheng,Z., Dai,Q. and Wang,H. (2019) Transfer RNA demethylase ALKBH3 promotes cancer progression via induction of tRNA-derived small RNAs. *Nucleic Acids Res.*, **47**, 2533–2545.
36. Ozanick,S., Krecic,A., Andersland,J. and Anderson,J.T. (2005) The bipartite structure of the tRNA m1A58 methyltransferase from s. cerevisiae is conserved in humans. *RNA*, **11**, 1281–1290.
37. Finer-Moore,J., Czudnochowski,N., O'Connell,J.D. 3rd, Wang,A.L. and Stroud,R.M. (2015) Crystal structure of the human tRNA m(1)A58 Methyltransferase-trna(3)(Lys) complex: refolding of substrate tRNA allows access to the methylation target. *J. Mol. Biol.*, **427**, 3862–3876.
38. Liu,J., Yue,Y., Han,D., Wang,X., Fu,Y., Zhang,L., Jia,G., Yu,M., Lu,Z., Deng,X. *et al.* (2014) A METTL3-METTL14 complex mediates mammalian nuclear RNA N(6)-adenosine methylation. *Nat. Chem. Biol.*, **10**, 93–95.
39. Wang,X., Feng,J., Xue,Y., Guan,Z., Zhang,D., Liu,Z., Gong,Z., Wang,Q., Huang,J., Tang,C. *et al.* (2016) Structural basis of N(6)-adenosine methylation by the METTL3-METTL14 complex. *Nature*, **534**, 575–578.
40. van Tran,N., Ernst,F.G.M., Hawley,B.R., Zorbas,C., Ulryck,N., Hackert,P., Bohnsack,K.E., Bohnsack,M.T., Jaffrey,S.R., Graille,M. *et al.* (2019) The human 18S rRNA m6A methyltransferase METTL5 is stabilized by TRMT112. *Nucleic Acids Res.*, **47**, 7719–7733.
41. Warda,A.S., Kretschmer,J., Hackert,P., Lenz,C., Urlaub,H., Hobartner,C., Sloan,K.E. and Bohnsack,M.T. (2017) Human METTL16 is a N(6)-methyladenosine (m(6)A) methyltransferase that targets pre-mRNAs and various non-coding RNAs. *EMBO Rep.*, **18**, 2004–2014.
42. Doxtader,K.A., Wang,P., Scarborough,A.M., Seo,D., Conrad,N.K. and Nam,Y. (2018) Structural basis for regulation of METTL16, an S-adenosylmethionine homeostasis factor. *Mol. Cell*, **71**, 1001–1011.
43. Pendleton,K.E., Chen,B., Liu,K., Hunter,O.V., Xie,Y., Tu,B.P. and Conrad,N.K. (2017) The U6 snRNA m(6)A methyltransferase METTL16 regulates SAM synthetase intron retention. *Cell*, **169**, 824–835.
44. Howell,N.W., Jora,M., Jepson,B.F., Limbach,P.A. and Jackman,J.E. (2019) Distinct substrate specificities of the human tRNA methyltransferases TRMT10A and TRMT10B. *RNA*, **25**, 1366–1376.
45. Finer-Moore,J., Czudnochowski,N., O'Connell,J.D., Wang,A.L. and Stroud,R.M. (2015) Crystal structure of the human tRNA m(1)A58 Methyltransferase-tRNA(3)(Lys) complex: refolding of substrate tRNA allows access to the methylation target. *J. Mol. Biol.*, **427**, 3862–3876.
46. Ueda,Y., Ooshio,I., Fusamae,Y., Kitae,K., Kawaguchi,M., Jingushi,K., Hase,H., Harada,K., Hirata,K. and Tsujikawa,K. (2017) AlkB homolog 3-mediated tRNA demethylation promotes protein synthesis in cancer cells. *Sci. Rep.*, **7**, 42271.
47. Thapar,R., Bacolla,A., Oyeniran,C., Brickner,J.R., Chinnam,N.B., Mosammaparast,N. and Tainer,J.A. (2019) RNA modifications: reversal mechanisms and cancer. *Biochemistry*, **58**, 312–329.
48. Xu,L., Liu,X., Sheng,N., Oo,K.S., Liang,J., Chionh,Y.H., Xu,J., Ye,F., Gao,Y.G., Dedon,P.C. *et al.* (2017) Three distinct 3-methylcytidine (m3C) methyltransferases modify tRNA and mRNA in mice and humans. *J. Biol. Chem.*, **292**, 14695–14703.
49. van den Born,E., Omelchenko,M.V., Bekkelund,A., Leihne,V., Koonin,E.V., Dolja,V.V. and Falnes,P.O. (2008) Viral AlkB proteins repair RNA damage by oxidative demethylation. *Nucleic Acids Res.*, **36**, 5451–5461.
50. Cheng,M.Y., You,X.J., Ding,J.H., Dai,Y., Chen,M.Y., Yuan,B.F. and Feng,Y.Q. (2021) Novel dual methylation of cytidines in the RNA of mammals. *Chem. Sci.*, **12**, 8149–8156.
51. Cheng,Q.Y., Xiong,J., Ma,C.J., Dai,Y., Ding,J.H., Liu,F.L., Yuan,B.F. and Feng,Y.Q. (2020) Chemical tagging for sensitive determination of uridine modifications in RNA. *Chem. Sci.*, **11**, 1878–1891.
52. Feng,Y., Chen,J.J., Xie,N.B., Ding,J.H., You,X.J., Tao,W.B., Zhang,X., Yi,C., Zhou,X., Yuan,B.F. *et al.* (2021) Direct

decarboxylation of Ten-eleven translocation-produced 5-carboxylcytosine in mammalian genomes forms a new mechanism for active DNA demethylation. *Chem. Sci.*, **12**, 11322–11329.
53. Wurtmann,E.J. and Wolin,S.L. (2009) RNA under attack: cellular handling of RNA damage. *Crit. Rev. Biochem. Mol. Biol.*, **44**, 34–49.
54. Fleming,A.M., Zhu,J., Howpay Manage,S.A. and Burrows,C.J. (2019) Human NEIL3 gene expression regulated by epigenetic-like oxidative DNA modification. *J. Am. Chem. Soc.*, **141**, 11036–11049.
55. Seok,H., Lee,H., Lee,S., Ahn,S.H., Lee,H.S., Kim,G.D., Peak,J., Park,J., Cho,Y.K., Jeong,Y. *et al.* (2020) Position-specific oxidation of miR-1 encodes cardiac hypertrophy. *Nature*, **584**, 279–285.